

Population Pharmacokinetic Modeling of VL-2397, a Novel Systemic Antifungal Agent: Analysis of a Single and Multiple Dose Phase 1 Study

L. L. Kovanda^{1,2}, S. M. Sullivan³, L. R. Smith³, P. Bonate², W. W. Hope¹¹ Molecular and Clinical Pharmacology Department, Institute of Translational Medicine, University of Liverpool, United Kingdom.² Astellas Pharma Global Development, Inc, Northbrook, IL, USA.³ Vical Inc, San Diego, CA, USA.

INTRODUCTION

- Invasive aspergillosis (IA) is a rapidly life-threatening fungal disease that most commonly affects patients with significant immunodeficiency¹.
- There is an urgent need to develop new antifungal agents with novel mechanisms of action (MOA) due to toxicity, drug-drug interactions, and increasing drug resistance incurred by existing antifungal agents.
- VL-2397 is a natural product isolated from *Acremonium persicinum*, strain MF-34733^{2,3} that is actively transported in fungi by siderophore iron transporter 1, a protein specifically produced by fungal but not mammalian cells.
- VL-2397 demonstrates rapid (within the first 2-4 hours) and potent *in vitro* fungicidal activity (MIC₉₀ values ≤ 2 mg/L) against *Aspergillus fumigatus* (including triazole-resistant *A. fumigatus*), *A. terreus*, *A. flavus*, *A. nidulans*, *Candida glabrata*, *C. kefyr*, *Cryptococcus neoformans*, and *Trichosporon asahii*.
- A first-in-human Phase 1 clinical trial with VL-2397 (VL2397-101) has been completed. Herein, we describe the population PK from this study, which was a randomized, dose-ranging, double-blind, placebo-controlled study to assess safety, tolerability and pharmacokinetics (PK) of intravenous infusion of VL-2397 to normal healthy subjects.

METHODS

- Study design:** Healthy adults in single ascending dose (SAD) Cohorts 1-7 received a single dose of VL-2397 ranging from 3 mg to 1200 mg. Subjects in multiple ascending dose (MAD) Cohorts 8-10 received multiple dosages of 300, 600, or 1200 mg once-daily for 7 days, while Cohort 11 received 300 mg every 8 hours (q8h) for 7 days followed by 600 mg every 24 hours (q24h) for the next 21 days. Infusion times varied with each regimen and ranged from 6 to 240 minutes.

- Pharmacokinetic Sampling:** The plasma sampling days and times are outlined in **Table 1**.

Table 1. Sampling Days and times by Cohort.

Cohorts	Day (s)	Pre-Dose	Mid-way through infusion	End of infusion	15 & 30 minutes*	Hours*	Days post-dosing
SAD 1-7	1	x	x	x	x	1, 2, 3, 4, 6, 8, 12, 24	36, 48
MAD 8-10	1	x	x	x	x	1, 2, 3, 4, 6, 8, 12, 24	36, 48
	3, 4, 5, 6	x	x	x	x	1, 2, 3, 4, 6, 8, 12, 24	36, 48
MAD 11	7	x	x	x	x	1, 2, 3, 4, 6, 8, 12, 24	36, 48
	1	x	x	x	x	3, 7, 8, 11, 15, 16, 19	32 and 38
	2, 3, 4, 5, 6	x	x	x	x	1, 2, 3, 4, 6, 8, 12, 24	36, 48
	7	x	x	x	x	3, 7, 8, 11, 15, 16, 19	32 and 38
	8, 9, 10, 15, 22	x	x	x	x	1, 2, 3, 4, 6, 8, 12, 24	36, 48
	28	x	x	x	x	1, 2, 3, 4, 6, 8, 12, 24	36, 48

*relative to the start of the infusion

- Bioanalytical Analysis:** VL-2397 plasma concentrations were determined using high performance liquid chromatography-tandem mass spectrometry (HPLC-MS/MS). The analysis was performed by MicroConstants (San Diego, CA, USA).
- Population PK (PPK) modeling:** Plasma concentrations were plotted over time as observed values and normalized values by daily dose.
- Plasma concentrations were used to construct a PPK model using Pmetrics® (U of Southern California, CA, v. 1.5.1)⁴. The plasma concentration data were weighted by the inverse of the estimated assay variance.
- Total drug was separated into two distinct compartments, (1) central compartment represents free unbound drug and (2) binding compartment represents bound drug. Measured drug concentrations are the sum of the bound and free compartments divided by the volume of the central compartment, i.e. $(X(1)+X(3))/V$.
- A degradation component (K_{deg}) was added to the binding compartment to address the irreversible loss of drug from that compartment.
- The mathematical formula of the saturable binding model is shown:

$$XP(1) = RATEIV(1) \cdot K_{on} \cdot X(1) + K_{pc} \cdot X(2) - CL/V \cdot X(1) - (K_{off}/10^6) \cdot (R_{tot} * 10^4) \cdot X(3) \cdot X(1) + (K_{off}/10^6) \cdot X(3) \cdot K_{cp} \cdot X(1) + K_{deg} \cdot X(4)$$

$$XP(2) = K_{cp} \cdot X(1) - K_{pc} \cdot X(2)$$

$$XP(3) = (K_{on}/10^6) \cdot (R_{tot} * 10^4) \cdot X(3) \cdot X(1) - (K_{off}/10^6) \cdot X(3) \cdot K_{deg}$$

$$XP(4) = K_{cp} \cdot X(1) - K_{pc} \cdot X(4)$$
- where K_{cp} , K_{pc} , K_{cp} , and K_{deg} = first-order intercompartmental rate constants (c, central; p, peripheral 2; f, peripheral 3 compartments). K_{on} and K_{off} = constants for the rates of association and dissociation, respectively. R_{tot} = maximum binding (in moles). K_{deg} = constant in the binding compartment (3), which regulates the slow turnover of the binding site and irreversible loss of drug from that compartment.
- Model acceptance:** Visual inspection of the observed-versus-predicted concentration values before and after the Bayesian step and the coefficient of determination (r^2) from the linear regression of the observed-versus-predicted values, and estimates for bias (mean weighted error) and imprecision (adjusted mean weighted squared error).
- Estimates of exposure:** Area under the concentration time curve for the first 24-hours (AUC_{0-24}) for all subjects and hours 144-168 ($AUC_{144-168}$) for MAD subjects were calculated using the Bayesian estimates from the final model using trapezoidal rule in Pmetrics.

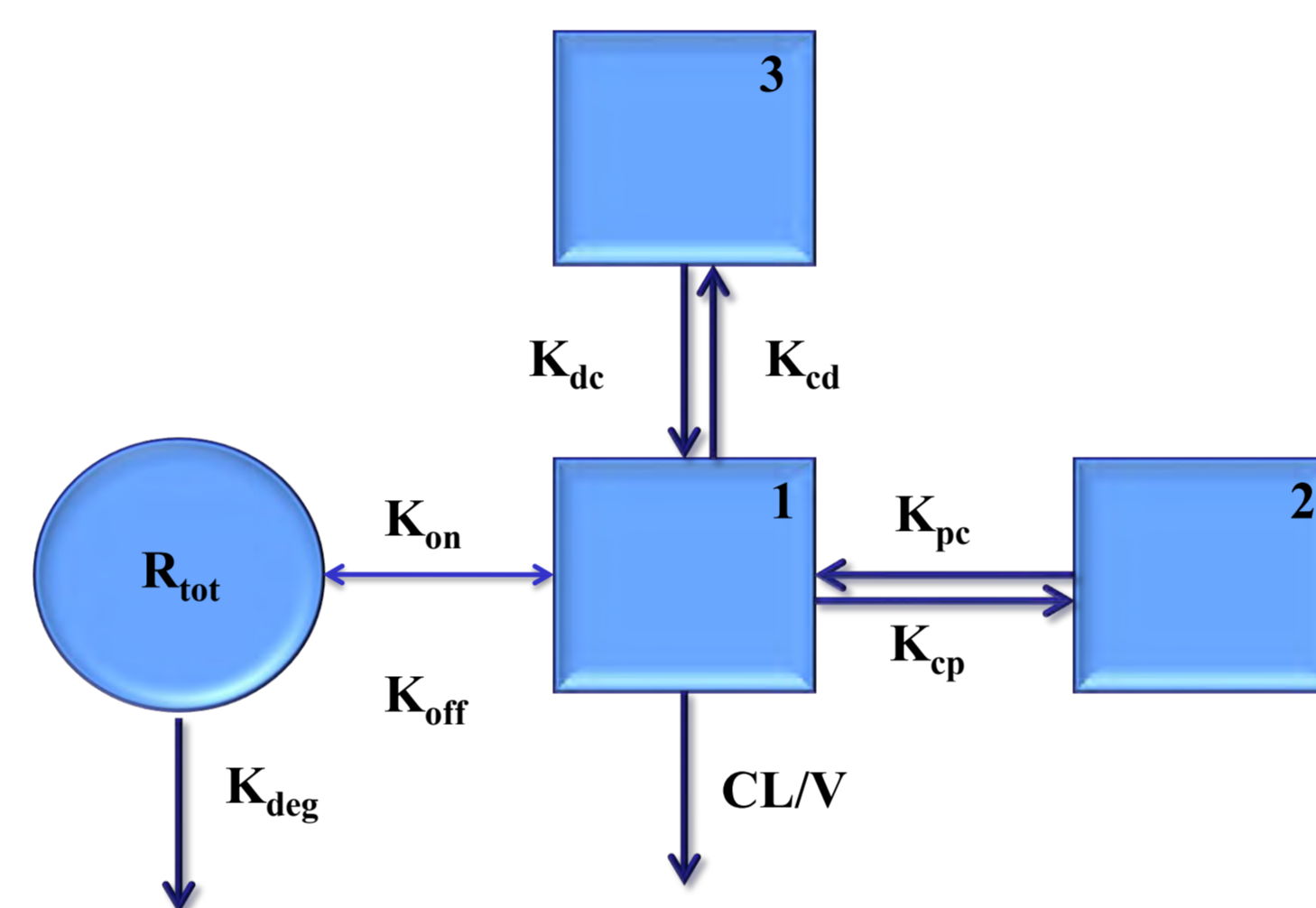
RESULTS

- Study Population:** 66 healthy subjects from 11 cohorts were included. The majority of the subjects were Caucasian (53, 80%).

Table 2. Demographics

	Age (yr)	Weight (kg)	Height (cm)	BMI (kg/m ²)	BSA (m ²)
median	43	74.2	168.2	26.7	1.8
range	21-55	56.5-109.3	146.8-195.1	20.1-30	1.5-2.4

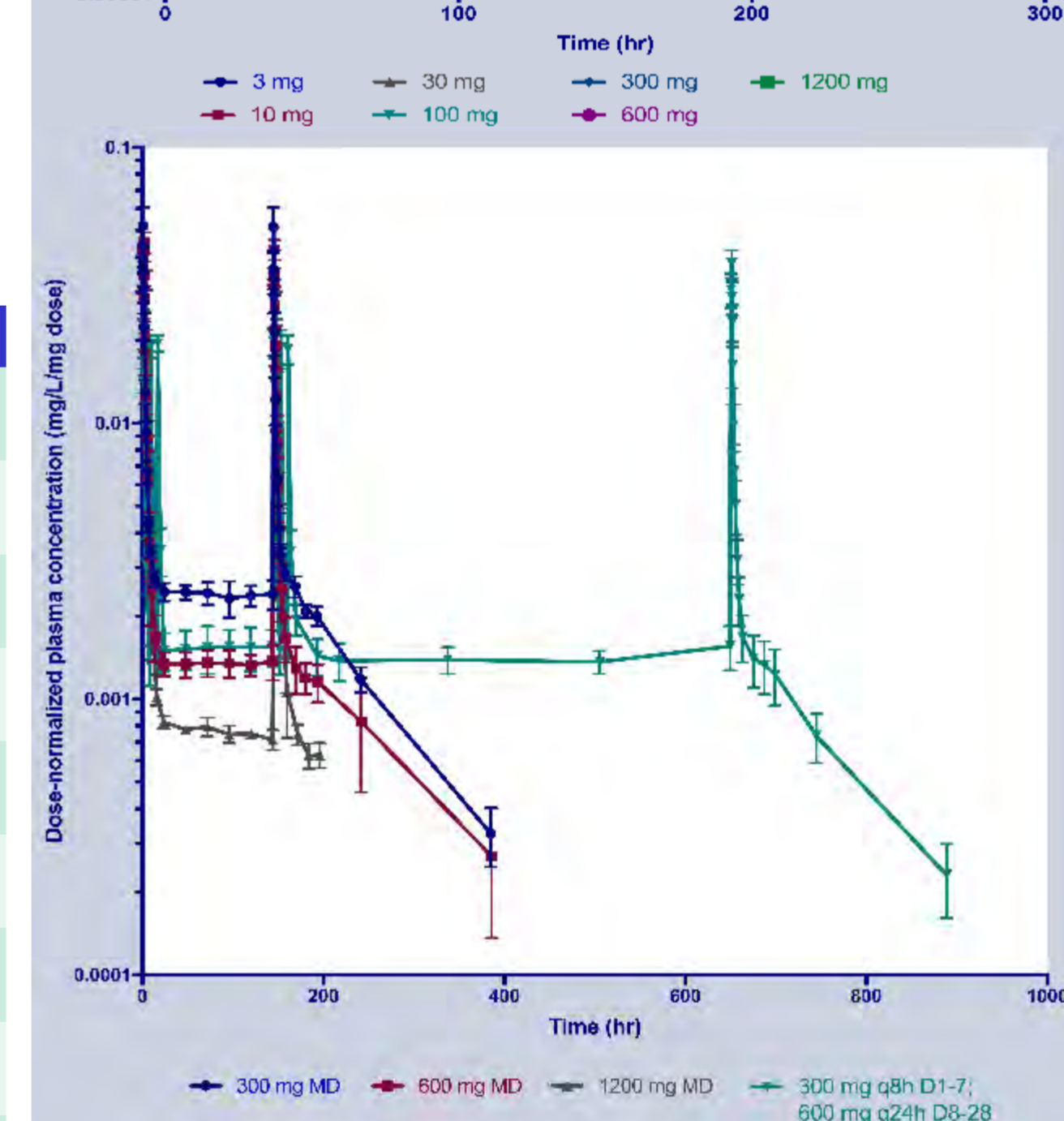
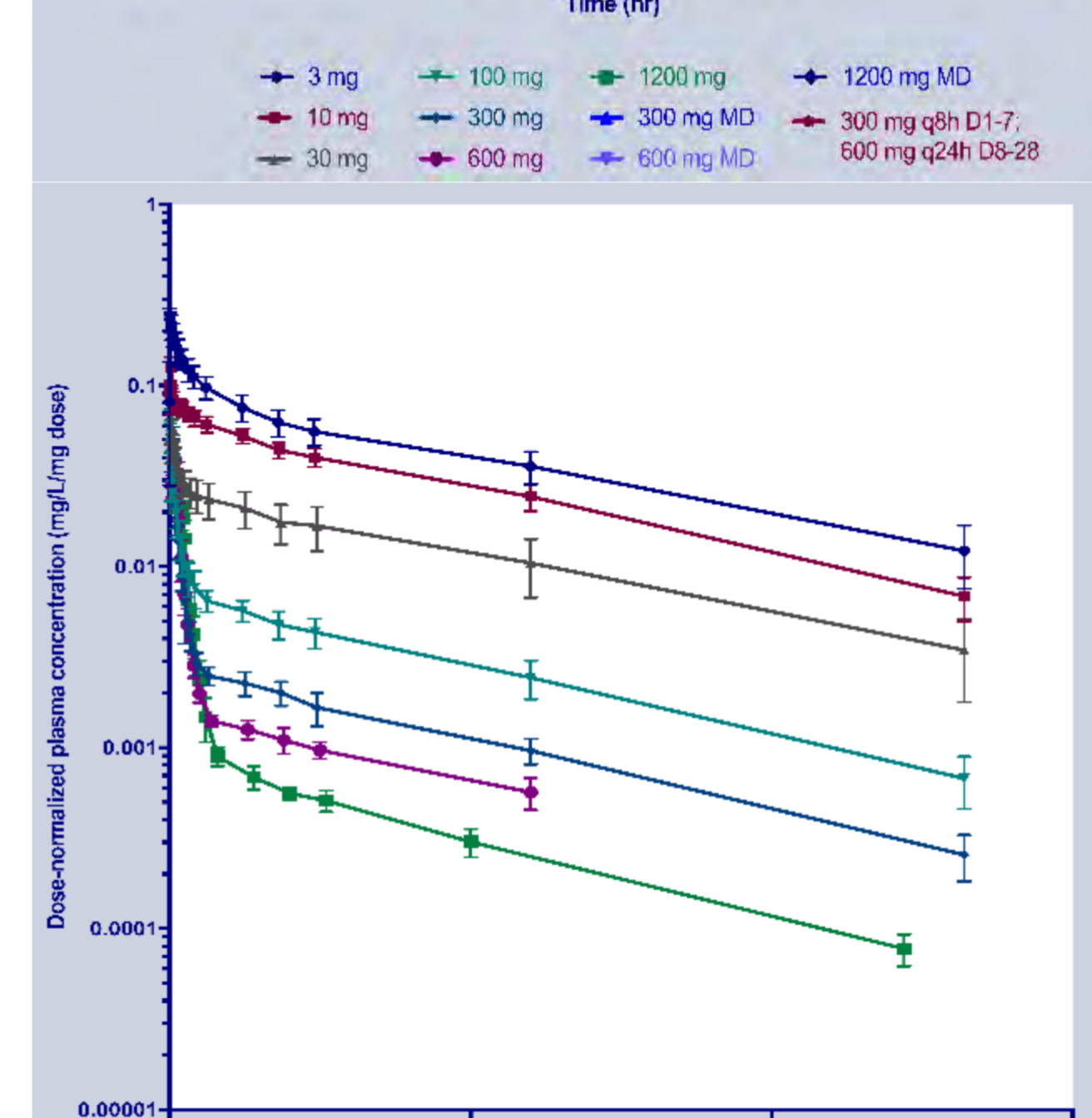
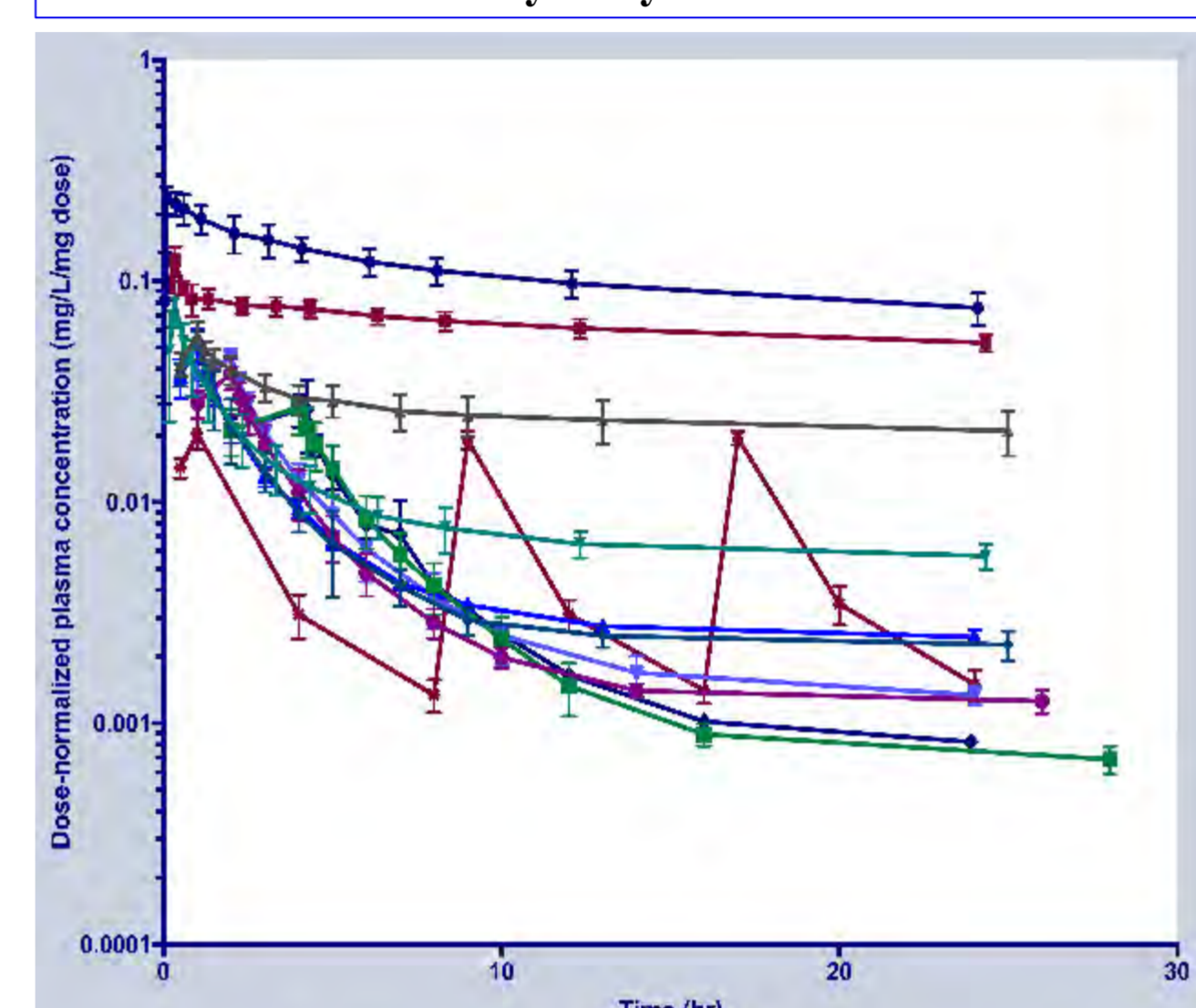
- Plasma Concentrations:** 1908 plasma concentrations were available for analysis. Concentrations did not increase proportionally with dose. The plasma concentration-versus-time curve demonstrated a rapid and saturable distribution phase.
- Dose-normalizing values show minimal overlap of these plots suggesting non-linearity, especially above dosages of 30 mg per day (**Figure 1**).
- Population PK Modeling:** A non-linear saturable binding model with 3 compartments fit the data well. The structural model is illustrated in **Figure 2**.

Figure 2. Illustration of structural PK model


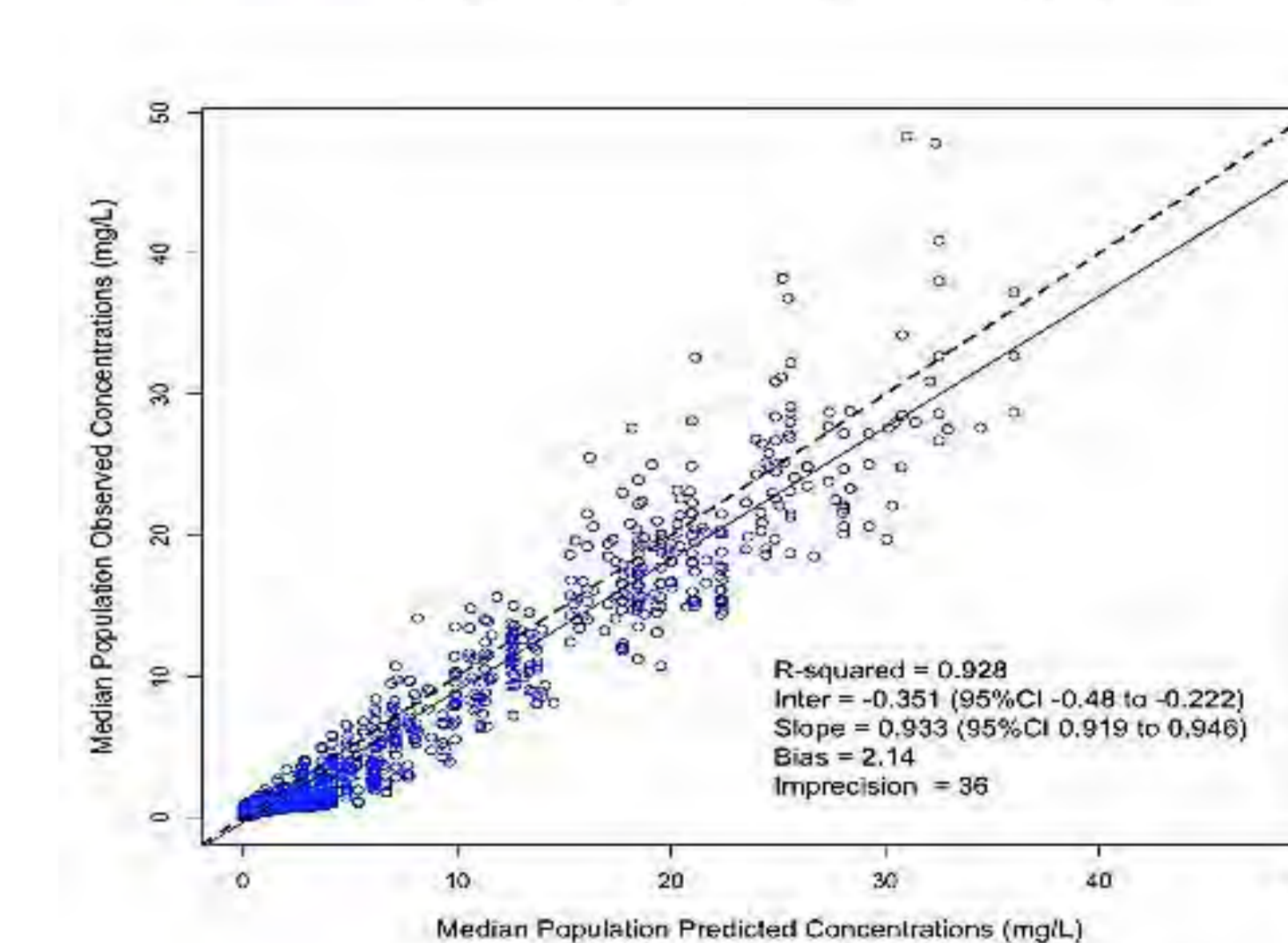
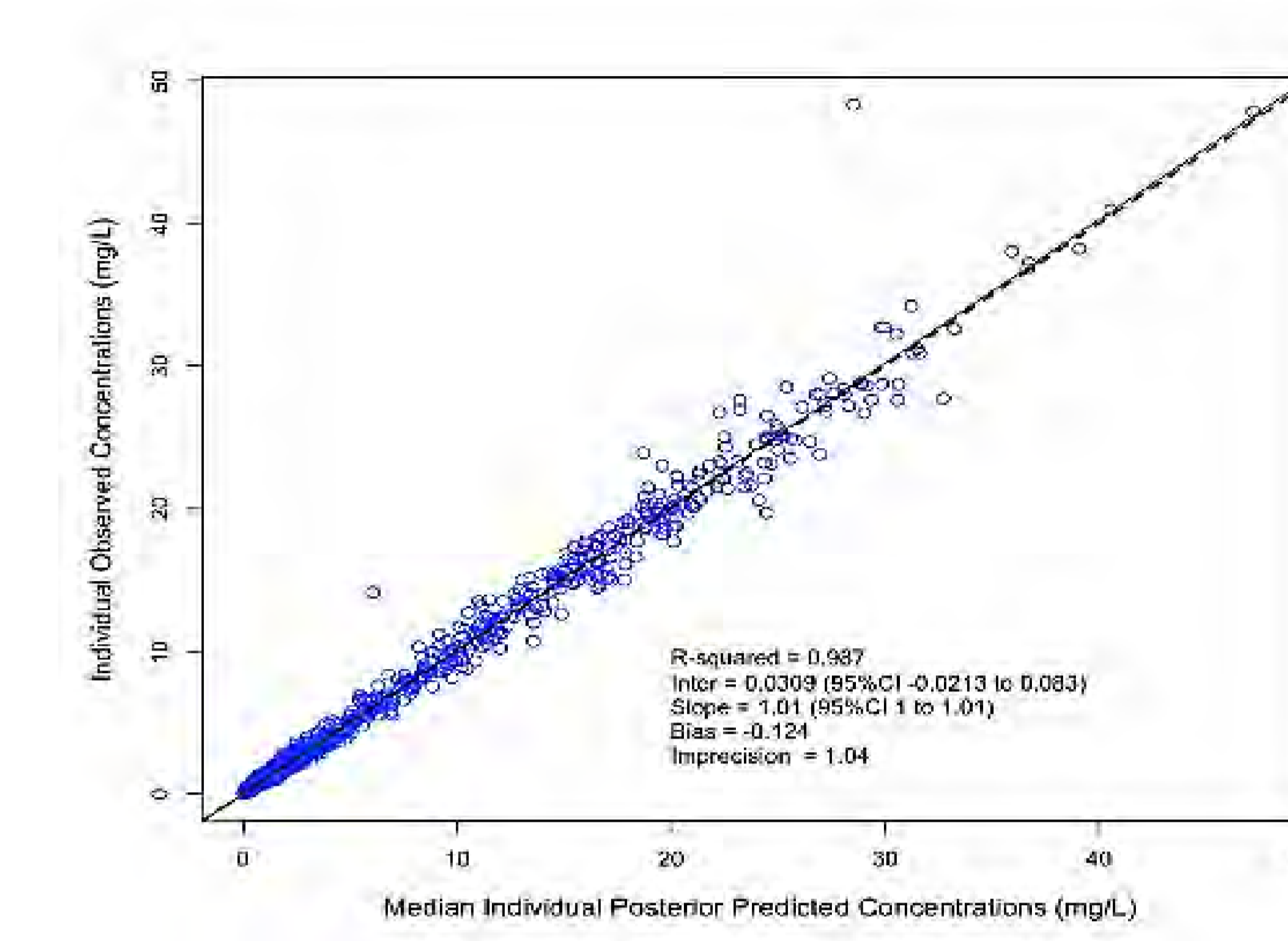
- Visual inspection of the observed-versus-posterior predicted concentrations after the Bayesian step was acceptable with a coefficient of determination (r^2) of 0.987 (slope = 1.01 [95% confidence interval 1 to 1.01]) (**Figure 3**). Measures of bias and imprecision were acceptable (-0.124 and 1.04, respectively).
- The estimated model parameters and simulated AUC values are included in **Table 3** and **4**, respectively.

Table 3. Parameter Estimates

	Mean	Population SD	Median	Range
CL/F (L/h)	5.56	3.57	6.80	0.25-9.95
V (L)	6.68	2.58	6.10	3.50-14.80
K_{cp} (hr ⁻¹)	2.31	1.75	2.45	0.025-4.98
K_{pc} (hr ⁻¹)	2.86	1.83	2.68	0.04-5.97
K_{on} (hr ⁻¹)	0.57×10^{-6}	0.44×10^{-6}	0.35×10^{-6}	0.008×10^{-6} - 1.49×10^{-6}
K_{off} (hr ⁻¹)	21.01×10^{-6}	20.25×10^{-6}	10.33×10^{-6}	0.35×10^{-6} - 49.75×10^{-6}
R_{tot} (mol)	1.79×10^4	1.25×10^4	1.46×10^4	0.52×10^4 - 3.98×10^4
K_{cp} (hr ⁻¹)	0.50	0.35	0.45	0.06-1.42
K_{pc} (hr ⁻¹)	0.69	0.90	0.22	0.02-2.99
K_{deg} (hr ⁻¹)	0.010	0.010	0.010	0.0003-0.050

Figure 1. Plasma concentrations over time normalized by daily dose


Top: All cohorts over first 24 hours. Middle: SAD Cohorts 1-6. Bottom: MAD Cohorts 7-11.

Figure 3. Illustration of structural PK model

Table 4. AUC values estimated from the PPK for each Dose Cohort

Cohort (dose)	AUC ₀₋₂₄ (mg-h/L)	AUC ₁₄₄₋₁₆₈ (mg-h/L)
1 (3 mg)	27.1 (4.2)	
2 (10 mg)	70.1 (7.6)	
3 (30 mg)	80.8 (24.9)	
4 (100 mg)	83.6 (28.8)	
5 (300 mg)	104.3 (12.8)	
6 (600 mg)	150.6 (17.7)	
7 (1200 mg)	236.0 (46.7)	
8 (300 mg)	319.9 (26.5)	133.1 (6.3)
9 (600 mg)	711.2 (104.5)	206.1 (24.9)
10 (1200 mg)	1352.1 (801.6)	302.6 (17.7)
11 (300 mg q8h D1-7; 600 mg q24h D8-28)	856.51 (120.0)	1237.2 (127.0)

*AUC₁₄₄₋₁₆₈ is only applicable to the multiple dose Cohorts (8, 9, 10, and 11)

CONCLUSIONS

- VL-2397 is a systemic antifungal agent in development for the treatment of IA and is one of few agents in development with a novel MOA that has the potential to overcome some of the deficiencies of currently licensed agents.
- Non-linear saturable binding kinetics best described the plasma concentration data.
- We hypothesize the source of the non-linearity is most likely due to saturable protein binding.
- The PPK model can now be used to optimize dosing by bridging the kinetics to efficacious pharmacodynamic targets.

- Cadena J, Thompson Gr, Patterson T. 2016. Invasive Aspergillosis: Current Strategies for Diagnosis and Management. Infect Dis Clin North Am 30:125-142.
- Nakamura I, Yoshimura S, Masaki T, Takase S, Ohsumi K, Hashimoto M, Furukawa S, Fujie A. 2017. ASP2397: a novel antifungal agent produced by *Acremonium persicinum* MF-347833. J Antibiot (Tokyo) 70:45-51.
- Nakamura I, Kanasaki R, Yoshikawa K, Furukawa S, Fujie A, Hamamoto H, Sekimizu K. 2017. Discovery of a new antifungal agent ASP2397 using a silkworm model of *Aspergillus fumigatus* infection. The Journal of Antibiotics 70:41-44.
- Neely MN, van Guilder MG, Yamada WM, Schumitzky A, Jelliffe RW. 2012. Accurate detection of outliers and subpopulations with Pmetrics, a nonparametric and parametric pharmacometric modeling and simulation package for R. Ther Drug Monit 34:467-476.